Published in final edited form as:
J Appl Physiol. 2007 September ; 103(3): 883–894.

PULMONARY PERFUSION IN THE PRONE AND SUPINE POSTURES IN THE NORMAL HUMAN LUNG

G. Kim Prisk[1,2], **Kei Yamada**[3], **A. Cortney Henderson**[1], **Tatsuya J. Arai**[1], **David L. Levin**[2,*], **Richard B. Buxton**[2], and **Susan R. Hopkins**[1,2]

1 *Department of Medicine, University of California, San Diego, La Jolla CA, 92093*

2 *Department of Radiology, University of California, San Diego, La Jolla CA, 92093*

3 *School of Medicine, University of California, San Diego, La Jolla CA, 92093*

Abstract

Prone posture increases cardiac output and improves pulmonary gas exchange. We hypothesized that in the supine posture, greater compression of dependent lung limits regional blood flow. To test this, MRI-based measures of regional lung density, MRI arterial spin labeling quantification of pulmonary perfusion, and density-normalized perfusion were made in 6 healthy subjects. Measurements were made in both the prone and supine posture at FRC. Data were acquired in 3 non-overlapping 15mm sagittal slices covering most of the right lung: central, middle and lateral, which were further divided into vertical zones: anterior, intermediate and posterior. The density of the entire lung was not different between prone and supine, but the increase in lung density in the anterior lung with prone posture was less than the decrease in the posterior lung (change: +0.07 g/cm^3 anterior, −0.11 posterior; P<0.0001) indicating greater compression of dependent lung in supine posture, principally in the central lung slice (P<0.0001). Overall density-normalized perfusion was significantly greater in prone posture (7.9±3.6 ml/min/g prone, 5.1±1.8 supine, a 55% increase, P<0.05) and showed the largest increase in the posterior lung as it became non-dependent (change: +71% posterior, +58% intermediate, +31% anterior, P=0.08), most marked in the central lung slice (P<0.05). These data indicate that central posterior portions of the lung are more compressed in the supine posture, likely by the heart and adjacent structures, than are central anterior portions in the prone, and that this limits regional perfusion in the supine posture.

Keywords

Prone; supine; MRI; lung density; gas exchange; gravity

INTRODUCTION

In the healthy lung it has generally been shown that the normally present gravitational gradients in pulmonary perfusion are smaller in the prone than in the supine posture (26;29), although the findings are not universal (2;17;28). Cardiac output and pulmonary diffusing capacity are increased slightly in the prone posture compared to supine with the difference being more pronounced under increased gravitational force (37), which also result in alterations in the distribution of pulmonary blood flow (33). This has lead to the suggestion that the mechanism of improved oxygenation in the prone posture in some critically ill patients is the elimination of compression of dependent lung regions thought to occur in the supine position. (8;20;27;

Address for Correspondence: G. Kim Prisk Ph.D., D.Sc., Department of Medicine, 0931, University of California, San Diego, 9500 Gilman Drive, La Jolla, CA 92093-0931, Phone 858-455-4756, FAX 858-455-4765, kprisk@ucsd.edu.
*Current address for D.L. Levin: Department of Radiology, Mayo Clinic, Rochester, MN 55905

30;40) As the lung becomes “heavier” either as a result of the accumulation of edema (such as in ARDS) or because of an increase in gravity (as in centrifuge experiments), this compressive effect is thought to be more pronounced, compromising blood flow to those regions (4;10; 31).

Studies in animal models using injected microspheres with subsequent excision and drying of the lung, have also shown small differences between the prone and supine postures (11) with less pronounced, or absent, vertical gradients in blood flow in the prone position. However, the post-mortem inflation of the lung in microsphere measurements serves to minimize any gravitational gradient in perfusion that is present (7), and thus may not entirely reflect the effect in the intact human lung. We recently showed that by taking into consideration the effects of lung compression in the supine lung using MRI techniques, we could reproduce both the gravitational gradient in perfusion typically seen in the *in-situ* lung (43), and the very much attenuated gradient seen in *post-mortem* studies that include post-excision lung inflation in the tissue processing (11); (16). In essence, if the lung is considered as a deformable structure in which much of the self-weight is due to the flowing blood, then correcting for the resulting density gradient transforms measurements of perfusion into measurements more akin to those obtained by microsphere studies, where density is more uniform.

Based on these prior studies we applied the same MRI techniques to study the changes in normal humans moved from the supine to the prone posture. We hypothesized that in the supine posture, compression of the most gravitationally dependent lung regions by the mediastinum and heart would result in an exaggerated gradient in pulmonary perfusion when compared to the prone posture. To be sure that any potential changes in perfusion were not solely as a consequence of the greater number of capillaries in a given volume of lung, the Slinky effect (16), we normalized perfusion for regional lung density. To explore this we performed MRI-based studies of both pulmonary perfusion and lung density in normal subjects in both the supine and prone postures with measurements made at FRC. The results show that the density gradients present in the prone posture are comparable to those in the supine posture, but there is evidence for dependent lung compression in the central part of the supine lung. Removal of this compression results in a significantly greater density-normalized perfusion of the lung when in the prone posture.

METHODS

Subjects

This study was approved by the Human Subjects Research Protection Program of the University of California, San Diego. Six healthy subjects (4 male, 2 female) aged 25±1 yrs, weight 74±8 kg participated in this study after giving informed consent, and undergoing screening using a pulmonary and MRI safety questionnaire, and undergoing a medical history and physical exam. These are the same six subjects studied in a previous publication (16). Some of the supine data reported here were also used in that publication to examine the effect of lung density gradients on the interpretation of regional perfusion data.

Imaging

Each subject underwent MRI scanning using a Magnetom Vision 1.5 Tesla whole-body MR Scanner (Siemens Medical Systems, Erlangen, Germany). All sequence parameters were kept within U.S. Food and Drug Administration guidelines for clinical magnetic resonance examinations. Subjects were positioned supine in the scanner, with a custom designed rigid PVC tubing cage positioned over the torso. The phased-array torso coil was positioned on this frame ensuring a constant distance between the anterior and posterior elements of the torso coil. A water phantom doped with gadolinium (Berlex Imaging, Magnevist®, 469 mg/mL

gadopentetate dimeglumine, 1:5500 dilution) to T_1 and T_2 values approximating that of blood, was placed next to the subject within the field of view for absolute quantification of pulmonary perfusion and proton density (see below). After allowing ~10 minutes to establish steady state, perfusion, lung density and coil correction data (all described below) were acquired by imaging the right lung in the sagittal plane, to eliminate imaging artifacts from the aorta and heart present within the left hemithorax. Sequential 15 mm slices were obtained during a 8–10 second breath-hold at functional residual capacity starting in the central lung adjacent to the heart and progressing laterally until signal intensity was reduced to less than 50% of baseline or until the imaging plane included the lateral chest wall. This was accomplished in 3–5 slices for each subject, depending on lung size. Of these, the middle three slices were selected for each subject, or in the case where 4 slices were obtained, data from the most lateral slice was not used. After data were collected in the supine posture the subject was removed from the scanner, repositioned in the prone posture and the imaging was repeated ~40 minutes after the supine data collection started. The overall study duration was ~90 minutes for each subject. The details of the imaging protocol using in this study were extensively described in a recent publication (16) and so are only briefly covered here.

Correction for coil inhomogeneity—In order to maximize the signal to noise ratio in the pulmonary perfusion and proton density data (described below), a torso coil was used, which has substantially higher sensitivity than the body coil built into the scanner. Using paired density images from the homogenous body coil, and the inhomogeneous torso coil, we corrected all blood flow and density images for coil inhomogeneity with a maximum spatial frequency across the field of view of ~2 cycles on a subject by subject basis (16).

Lung perfusion imaging—Regional pulmonary blood flow was assessed using a 2D ASL-FAIRER sequence with a half-Fourier acquisition single-shot turbo spin-echo (HASTE) imaging scheme (see (3;16) for full details). Arterial spin labeling (ASL) exploits the capability of MRI to invert the magnetization of protons (primarily in water molecules) in a spatially selective way using a combination of radiofrequency pulses and spatial magnetic field gradient pulses. By inverting the magnetization of arterial blood, these “tagged” protons in blood act as an endogenous tracer. During each measurement two images are acquired during a single breath-hold of each lung slice with the signal of blood prepared in a different way. In one image, the magnetization of the blood both inside and outside the imaged section is inverted, resulting in very low signal from both blood and tissue when the image is acquired ~80% of one R-R interval later. In the second image the inversion is applied only to the imaged slice, resulting in any inflow of blood from outside that slice having a strong MR signal. When the two images are subtracted, canceling the stationary signal, the result is a quantitative map of blood delivered to the imaging plane from one systolic ejection period (3;16).

Data were obtained during a breath-hold at functional residual capacity in multiple 15-mm-thick sagittal slices. Each slice was 40cm × 40cm and imaged at a resolution of 256×128 pixels, therefore voxels of approximately 1.5 × 3 × 15 mm (~0.07cm ^{3}) were obtained. These ASL image files were later resized during post-processing to match the voxel size of the lung density images (3 × 3 × 15mm) using bilinear interpolation in MATLAB (The MathWorks, Inc, Natick, MA), giving an effective resolution of ~0.14 cm^3. The subtracted ASL image was corrected for coil inhomogeneity, and pulmonary blood flow was quantified in ml/min/cm^3 lung based on the doped water phantom contained within the field of view for each image.

Lung density imaging—In addition to the ASL images, a proton density image was acquired in the same sagittal slices using a 2D spoiled gradient recalled echo sequence (sometimes referred to as FLASH, Fast Low Angle Shot) during a separate breath-hold. Sequence parameters were repetition time (TR) = 6 msec, echo time (TE) = 0.9 msec, flip angle = 4°, slice thickness 15 mm, field of view (FOV) 40cm × 40cm, and image size 128×128 pixels.

The resulting proton density was then calculated by correcting the signal for the rapid T2* decay of signal from the lungs based on published values of T2* (1.43±0.41 msec, (13)). In each image so obtained, the resulting signal in each voxel, after correcting for coil inhomogeneity was related to the signal derived from the water phantom (which is by definition 100% water) to obtain regional lung proton (water) density in units of ml H_2O/cm^3 lung, subsequently referred to as lung density.

Density-normalized perfusion—Density-normalized perfusion expressed in units of ml/min/g water can be approximated by dividing the image acquired by ASL, which has the units of ml/min/cm^3 lung, by the image of lung density (in g H_2O/cm^3 lung). A mutual-information-based technique that included translation and rotation was utilized to register the two images (34), and the ASL image was divided by the density image on a voxel by voxel basis to give perfusion in ml/min/g using a custom designed program in MATLAB. To the extent that regional lung density (tissue + blood) is reflected by the water content, density-normalized perfusion then reflects perfusion in ml/min/g lung.

Data Analysis

Data representation—For each image acquired as described above (density, perfusion, and density-normalized perfusion) the data were analyzed in the following manner. For each image, mean, standard deviation and relative dispersion (standard deviation divide by mean) were calculated. The vertical distributions (distance above the most dependent portion of the lung for each subject) were plotted for each slice and posture for perfusion, lung density and density-normalized perfusion. Zero height was defined as the most dependent voxel of the lung in the three slices, and this reference was used for all slices in that image set. The relationship between vertical height and perfusion, density, and density-normalized perfusion was characterized using least squares linear regression and the slope and strength of the association (r^2) obtained. Since distributions of perfusion and density across gravitational distances may not necessarily be best expressed as a linear relationship, each sagittal slice was divided into three gravitationally-based regions of interest: dependent, intermediate, and non-dependent regions to allow for comparison between regions (see Figure 1). The slice with the greatest anterior to posterior height was selected from the three contiguous sagittal images and divided horizontally into three zones of equal height based on the maximum anterior-posterior dimension of the lung. The remaining two contiguous lung slices were divided into three zones using the same horizontal coordinates. Mean perfusion, density and density-normalized perfusion were obtained for each slice and zone in both the prone and supine postures.

Heterogeneity—As in previous studies, we used the relative dispersion (RD, the standard deviation divided by the mean, also known as the coefficient of variation) of each lung slice as a measure of the degree of heterogeneity. Relative dispersion is a good descriptor of the overall degree of heterogeneity present in an image. It has been shown to change under numerous circumstances (14;15;21) in a reproducible manner when applied to the distribution of pulmonary perfusion.

Statistical analysis—ANOVA (Statview, 5.0 SAS Institute Inc. Cary, North Carolina) for repeated measures was used to statistically evaluate changes in the major dependent variables over 3 repeated measures: 1) posture (2 levels: prone and supine), 2) lung slice (3 levels: central lung, middle lung, lateral lung) and 3) gravitational region (3 levels: nondependent, intermediate, dependent region). Dependent variables for this analysis were perfusion in units of ml/min/cm^3 of lung, lung density in units of g/cm^3 lung, and density-normalized perfusion in units of ml/min/g. Where overall significance occurred, post hoc testing was conducted using Student's t-testing. All data are presented as means ± SD, the null-hypothesis (no-effect) was rejected for $P < 0.05$, 2 tailed.

RESULTS

All subjects completed the study, and no data were discarded. Heart rate averaged 68 ± 13 bpm over the course of the study and was not significantly affected by posture (66 ± 12 supine, 70 ± 13 prone, P = 0.2). Mean arterial oxygen saturation measured by pulse oximetry did not change between prone and supine postures (97.4 ± 1.0 % for both postures, P = 0.86).

Table 1 presents the overall results of the study with the right lung considered in three sagittal slices (central, 'C'; middle, 'M'; and lateral, 'L'), each of which is in turn divided into three distinct vertical regions (posterior, 'P'; intermediate, 'I'; and anterior, 'A'). The slice selection and division of each slice into vertical subdivisions is detailed in the Methods section (above). For each of these subdivisions, the mean values of lung density (in g/cm^3), perfusion (in ml/min/cm^3) and density-normalized perfusion (in ml/min/g) are presented.

Density

Figure 2 shows an overall view of the effects of gravity and posture on lung density. Panels A and B show the vertical distribution of lung density in the supine and prone postures respectively, for each of the three sagittal lung slices. In these figures the solid lines represent the mean values for lung density in adjacent 1 cm high isogravitational planes (the x-axis) plotted as a function of height above the zero reference point (the y-axis). Thus for panel A, the data are shown with the most posterior lung plane at the bottom of the figure while for the data in panel B (prone posture), the data at the bottom of the figure are from the most anterior plane. Mean data from all three sagittal lung slices are shown in each panel. The shaded area is the region encompassing the mean ± SD values for the middle lung slice (labeled 'M') and provides a visual guide to the degree of variability in all lung slices, which is generally comparable between slices in terms of their SD values.

Gravitational zones—Averaged over postures and lung slices there was a highly significant difference (P<0.0005) in density between lung gravitational regions such that density was significantly less in the non-dependent gravitational regions and greater in the gravitationally dependent region. This can most easily be seen in Figure 2 panels C–E. In these panels data are presented on a gravitational basis for each of the three sagittal slices separately. In each panel the supine data are presented as mean with the area encompassing ± 1SD being shaded, and the prone data as the mean only. The bottom of the figure shows the most gravitationally dependent lung plane (supine, posterior; prone, anterior). In the non-dependent gravitational region (see also Table 1), lung density averaged 0.28 ± 0.10 g/cm^3 and this progressively increased in the intermediate (0.33 ± 0.09 g/cm^3, P<0.005 compared to non-dependent) and dependent (0.37 ± 0.10 g/cm^3, P<0.05 compared to intermediate) gravitational regions. Over the entire lung, these gravitational differences in lung density were not different between the different lung slices (P<0.32). The vertical gradient in density was unchanged (−0.038 ± 0.034 g/cm^3/cm height supine; −0.031 ± 0.043 g/cm^3/cm height prone; both different from zero (P<0.05); P=0.2 supine versus prone).

Posture—There were no significant differences in overall lung density between the prone posture (0.320 ± 0.106/cm^3) compared to supine (0.332 ± 0.102 g/cm^3) (P = 0.69, see Table 1). However, not unexpectedly, there were highly statistically significant changes with posture between the different gravitational regions (P<0.0001). For example, the posterior lung regions, which have the highest density in the supine posture, become the regions of lowest density in the prone posture. The intermediate regions of the lung did not change density significantly with a postural change (P = 0.89) (Table 1, Figure 3, panel A). There was a significant difference in these regional changes in density between lung slices (P<0.0001). The posterior-central and anterior-central lung showed the greatest change in density as they were

shifted from supine to prone posture (a −46 % and +25 % change respectively, P<0.0001), with the change in middle lung slice being slightly less marked (P<0.005) and there being very little change in the lateral lung slice (P = 0.2). This can also be in Figure 2 in panels C and D as greater density in the dependent 1/3 of the lung in central and medial lung slices in supine posture.

Heterogeneity of density—Overall density heterogeneity as measured by the relative dispersion averaged 0.33 ± 0.07 over all lung slices and postures. Heterogeneity of lung density was significantly different between lung slices (P <0.0005) and was least uniform in the central lung slice and progressively more uniform laterally. However there was no significant effect of posture on the density heterogeneity (P = 0.22).

Perfusion

Figure 4 shows the effects of gravity and posture on perfusion measured in ml/min/cm^3. The format is that of Figure 2 and the shaded areas provide a visual guide to the degree of variability in isogravitational lung zones.

Gravitational zones—Averaged over postures and lung slices there was a highly significant difference (P<0.0001) in perfusion between lung gravitational regions such that perfusion was significantly less in the non-dependent and dependent gravitational regions compared to the intermediate gravitational region (Table 1), which is also clearly visible in Figure 4. This was manifest as a vertical gradient in perfusion in both postures (−0.034 ± 0.07 ml/min/cm^3/cm of height supine, −0.025 ± 0.038 prone; both different from zero, P<0.05). In the intermediate gravitational zone, lung perfusion averaged 2.4 ± 1.0 ml/min/cm^3 and this was significantly greater than in either the nondependent (1.6 ± 0.7 ml/min/cm^3, p <0.0001) and dependent (1.9 ± 0.7 ml/min/cm^3, p<0.0005) gravitational regions which were also significantly different from one another (P<0.05). These gravitational differences were different between the different lung slices (P<0.0001) and were greatest in the central portion of the lung (Figure 4, panels C,D,E).

Posture—Overall, pulmonary perfusion was significantly affected by posture, with higher perfusion in the prone than the supine posture (supine 1.62 ± 0.69 ml/min/cm^3 vs prone 2.26 ± 0.92, P <0.05). In both postures there was significant less perfusion moving from the central to the lateral lung slice. In the central slice of the lung, perfusion averaged 2.4 ± 1.0 ml/min/cm^3 and this was progressively reduced in the middle (1.9 ± 0.8 ml/min/cm^3) and lateral (1.5 ± 0.6 ml/min/cm^3) lung slices (all P<0.05). This effect can be seen in Table 1, and is clearly visible in panel B of Figure 3, and in panels A and B of Figure 4. The postural changes were significantly different between the different gravitational regions (P<0.01): the posterior zone of the lung showed a small increase in perfusion as it was shifted from dependent to nondependent with the change in posture from supine to prone, however there were marked increases in perfusion in both the intermediate and the anterior zones of the lung, and perfusion to the most gravitationally non-dependent zone of the lung (anterior in the supine posture, posterior in the prone posture) was much higher in the prone than the supine posture (Table 1 and Figures 3 and 4). While there were differences in absolute values between postures for these zones, the overall picture between supine and prone is largely similar, with perfusion decreasing between central and lateral slices, and being highest in the intermediate lung zone in both postures.

Heterogeneity of perfusion—Overall perfusion heterogeneity as measured by the relative dispersion averaged 0.75 ± 0.22 over all lung slices and postures. Relative dispersion was significantly greater in the central lung slice (0.88 ± 0.19) and was progressively less (P<0.0001) in the middle (0.75 ± 0.20) and lateral slices (0.61 ± 0.18). There was no significant

difference in perfusion heterogeneity between postures (prone 0.72 ± 0.20, supine 0.78 ± 0.22, P = 0.41).

Density-normalized perfusion

Figure 5 shows the effects of gravity and posture on density-normalized perfusion measured in ml/min/g. The format is that of Figure 2 and the shaded areas provide a visual guide to the degree of variability in isogravitational lung zones.

Gravitational zones—Density-normalized perfusion averaged over postures and lung slices (Table 1) shows a significant difference in perfusion between lung gravitational regions ($P < 0.005$), such that the intermediate zone was significantly greater than the dependent zone, which in turn was greater than the nondependent zone (all $P<0.05$). The next effect of this was that in contrast to perfusion, density-normalized perfusion showed no vertical gradient in either posture (slope +0.032 ± 0.110 ml/min/g/cm of height supine; +0.010 ± 0.058 prone; neither significantly different compared to zero).

Posture—In keeping with the overall increase in perfusion and unchanged density, density-normalized perfusion was significantly greater in the prone posture (7.88 ± 3.55 ml/min/g) compared to supine (5.12 ± 1.75 ml/min/g) ($P<0.05$). In the supine posture, density-normalized perfusion was not different between slices moving from central to lateral (see Figure 5, panel A, and Table 1). In sharp contrast however, in the prone posture, there were marked increases in perfusion in both the central (8.93 ± 3.31 ml/min/gm prone, 5.37 ± 1.97 supine $P<0.04$) and middle (8.72 ± 3.59 ml/min/gm prone, 5.32 ± 1.78 supine $P<0.03$) lung slices compared to supine, which was not significant in the most lateral lung slice (5.98 ± 3.11 ml/min/gm prone, 4.68 ± 1.45 supine, $P<0.13$) (see Figure 3 panel C, and Figure 5 panels C–E).

Figure 5 (panels C, D, E) shows that in the prone posture the non-dependent lung zones (i.e. posterior lung) exhibited greater density-normalized perfusion than in the supine posture. This difference was only statistically significant ($P<0.01$) in the most central lung slice (Table 1, compare supine central anterior with prone central posterior). In contrast, dependent lung zones showed no difference between postures. Importantly, in the central and middle lung, density-normalized perfusion increased in the prone posture in all lung zone, with the largest increase being seen in the posterior lung (Figure 3, panel C).

Heterogeneity of density-normalized perfusion—Perfusion heterogeneity as measured by the relative dispersion averaged 0.69±0.18 over all lung slices and postures, and was comparable to the perfusion measurements expressed as a function of volume. As with the volume-based measurements, relative dispersion was significantly different between lung slices ($P=0.005$), with the central lung showing the greatest perfusion heterogeneity, and there was a significant posture by lung slice interaction ($P<0.05$), reflecting that this was observed only in the supine posture. In keeping with this, averaged over all the lung slices there were no significant changes in heterogeneity of density-normalized perfusion with different postures (0.71 ± 0.18 supine; 0.70 ± 0.12 prone; P = 0.77).

DISCUSSION

The overall aim of this study was to make measurements of the distribution of pulmonary perfusion and lung density in the normal lung. We hypothesized that the effects were largely mechanical in origin (i.e. a function of the effects of gravity itself on the lung and associated structures) as opposed to some active control mechanism(s). To study these effects we utilized recently developed techniques to quantitatively measure the spatial distributions of both pulmonary perfusion and lung density using MRI. The results show that the prone posture

results in an overall increase in pulmonary perfusion, and that this increase is manifested in the form of increased perfusion per alveolus in the gravitationally non-dependent regions of the lung compared to the supine posture.

Our results show that the prone posture was associated with a significant overall increase in perfusion of the right lung from 1.62 ml/min/cm^3 in the supine posture to 2.26 ml/min/cm^3 in the prone, a ~40% increase. This result is in keeping with a previous study (37) which also showed that pulmonary perfusion is increased in the prone versus supine posture, although the magnitude of the change we observed is larger. Our studies do not permit us to directly examine the mechanisms of such a change, however, it has been previously suggested that there is a negative hydrostatic gradient for venous return in the supine posture as more lung is dependent relative to the left atrium than in the prone posture (9), and that this might impair cardiac output (38;39). Further, our study examined only the right lung, and if greater compressive effects are present on the left side, as in the case in the compromised lung (1;23) then increases in flow to one lung may not be indicative of overall changes in cardiac output. Studies in ALI/ARDS have shown a similar overall cardiac output in both the prone and supine postures in humans (32) and in animals (19;36) despite improved arterial oxygenation in the prone posture. Thus the improvement in overall pulmonary perfusion in the prone posture is unlikely to contribute greatly to the improved gas exchange in that posture compared to supine.

Rohdin et al (37) saw a ~8% increase in FRC in the prone posture compared to supine, and suggested that this may have resulted in improved diastolic filling. We did not directly measure FRC in these studies, but the average number of voxels in our imaging volume attributed to lung was 3482 ± 848 supine and 3733 ± 451 prone. This ~7% change in this study was however not significant (P=0.57) and was not uniformly seen across all subjects.

Changes in perfusion distribution with posture

It has long been appreciated that gravity results in the deformation of the lung due to its own weight. In the 1960's, studies showed gravitational gradients in pulmonary ventilation and alveolar size (6;25), and numerous authors have referred to this mechanism and its effect on lung ventilation. What has been less-well appreciated is that this gravitational compression has direct and important effects on pulmonary perfusion. In a recent study using the same quantitative MRI techniques as those employed here, we showed that much of the apparent gravitational gradient in pulmonary perfusion measured on a per unit volume basis was a direct consequence of gravitationally-induced gradients in lung density. In essence, if one considers a lung that has perfectly uniform perfusion per alveolus, any effect that results in a gradient in alveolar size must necessarily result in a similar although reversed gradient in apparent perfusion of the lung when measured on a per unit volume basis, because the perfusion occurs within the walls of the alveoli. In this study, by measuring both density and perfusion, and calculating density-normalized perfusion, we were able to consider changes in blood flow changes without the confounding effects of any apparent alterations due to density changes alone. Considering pulmonary perfusion on a per unit lung weight basis, shows a much more uniform vertical distribution of blood flow than does perfusion on a per unit volume basis, and serves to shed light on the mechanism of improved gas exchange with prone positioning.

Figure 3 shows the changes in density (A), perfusion (B) and density-normalized perfusion (C) in each zone of the lung in all slices studied. The distribution of perfusion (in units of ml/min/cm^3) shows the increase in total perfusion discussed above in the prone position compared to supine, but the overall gravitational pattern of perfusion appears largely similar between postures (Figure 4). Perfusion is low in the most gravitationally dependent region of the lung (i.e. the posterior lung when supine or the anterior lung when prone), rises to a maximum at about 1/3 of total vertical lung height, and then falls to low levels in the uppermost portions of the lung (Figure 4 panels A and B). The effects of a change in posture from supine to prone

are best appreciated by considering the panels C-E in Figure 4, which show the effects of such a change in the central, middle and lateral slices respectively. Moving from the supine to prone posture results in an increase in perfusion in the intermediate lung zone in all slices of the lung (Figure 3 panel B), consistent with the overall increase in perfusion in the prone posture described above. In the central lung the anterior zone increased perfusion in the prone posture, consistent with a move to a gravitationally dependent position. In contrast however, there was no change in perfusion in the central posterior lung, suggesting that in the supine posture, this zone of the lung had limited perfusion, likely as a consequence of compression by adjacent structures (e.g. the heart, mediastinum, and abdominal contents). This speculation is supported by the large change in density in this part of the lung (Figure 3, panel A). The central posterior lung showed the largest reduction in density moving from supine to prone of any region, and the magnitude of this change was greater than the corresponding increase in density in the central anterior lung. The effect can also be appreciated by the higher values of perfusion in the upper regions of panels D and E of Figure 4.

In contrast, density-normalized perfusion (ml/min/g) (Figure 5) shows a different pattern to perfusion (ml/min/cm^3). In the supine posture, overall density-normalized perfusion was not different between lung slices (Figure 5, panel A) and was largely uniform down the lung except in the most dependent and non-dependent zones of the lung. The lack of a vertical gradient in density-normalized perfusion was previously observed (16) and this pattern is maintained moving laterally across the lung. In contrast, in the prone posture density-normalized perfusion is higher in the central and middle slices than in the lateral lung (Figure 5 panel B). A postural change from supine to prone resulted in a significant increase in density-normalized perfusion in both the central and middle lung slices (Figure 5 panels C and D), but not in the lateral slice (Figure 5 panel E). This increase occurred as a result of increased density-normalized perfusion in the most non-dependent zones of the lung, an effect that can also be appreciated in Table 1 and in Figure 3 panel C. When moving from supine to prone, the posterior zones show a much greater increase in density-normalized perfusion than do the anterior zones. The overall picture is that posterior zones in both the central and middle slices greatly increase density-normalized perfusion when moved from supine to prone, an effect likely due to the removal of compression of this part of the lung in the supine posture.

It is important to note that considering perfusion (Figure 3, panel B) does not lead to the same conclusion as the effect is masked by lung deformation due to gravity. In essence, the compression of dependent lung results in a higher capillary density per unit volume of lung. Thus, perfusion expressed on the basis of a unit of lung volume will appear greater in this region, even though blood flow per gram of lung tissue may be uniform (16). To some extent, density-normalized perfusion can be considered as a surrogate measure of perfusion per alveolus. The normal lung consists of lung tissue and blood (in approximately equal amounts (5)), and gas space. Since the lung tissue and blood form the alveolar walls, and since they are the only components of the lung density signal, a higher lung density signal will result from compressed lung (such as occurs in dependent lung zones). Similarly compressed lung zones also have a larger number of alveoli per unit volume (6). Our measurements of perfusion shows a pattern of blood flow distribution similar to that of Hakim et al. (12) who showed a central-to-peripheral gradient in perfusion in all directions. This is similar to that seen in Figure 4, where perfusion is greatest both centrally in the lateral direction, and in the anterior-posterior direction (Figures 4A and 4B). However such a pattern is not apparent when considering density-normalized perfusion (compare Figures 4A and 5A) suggesting that the central-to-Peripheral gradient is a consequence of lung density effects.

Lung density and compression of dependent lung

Lung density follows a largely similar pattern between the prone and supine postures. As expected, the lung becomes denser in the gravitationally dependent zones, and denser in the more central slices of the lung (Figure 2). This is likely a direct result of the gravitationally-induced compression of the lung which would be expected to produce a largely uniform increase in density as one moves lower, and the effect of the pulmonary vessels becoming smaller as one moves from a central to lateral position in the lung. For the most part the gradient in lung density was independent of posture, implying a simple gravitational dependence of density. There may also be some effect of lateral compression of the lung by the heart which would be expected to be greater in the supine posture than in the prone (22).

There was however, a small postural effect on the vertical gradient in lung density, with higher density in the most gravitationally dependent zones of the lung in the supine posture compared with the prone, mostly in the central lung slice (Figure 2, panel C). This is most clearly seen in Figure 3, panel A where the central posterior lung region shows the greatest change in density moving from supine to prone. We speculate that this is likely a result of the shape of the lung, which in the humans has a large caudal projection in the posterior zone. In the supine posture this zone of the lung will be subject to compression by the heart and mediastinal structures, in the central in middle slices. This effect may exacerbate the increase in density in this zone, an effect referred to by others in the past (18;29). While this effect is small (and likely of little physiological consequence) in these normal lungs, this does not rule out a significant compressive effect in dependent lung zones in the supine posture in lungs of higher density (such as might occur in ARDS).

The similar vertical gradient in density supine and prone is consistent with the previous study of Musch et al (28), but not with other studies which have shown greater density gradients in the supine posture compared to prone (17;24). We suggest that the latter results may have been influence by the presence of high compression regions (principally central posterior lung, Figure 3, panel A) which highlights the important local effects of adjacent structures.

Heterogeneity of pulmonary perfusion

Overall, the relative dispersion (RD, standard deviation divided by the mean) of perfusion did not alter between the prone and supine postures, whether considering perfusion or density-normalized perfusion. There was a small effect on RD of perfusion which decreased as one moved from a central to lateral position in the lung. When considering density-normalized perfusion, this effect was absent, suggesting it was related to the effects of the lung density. The fact that RD did not significantly alter in this study, despite clear differences in the distribution of perfusion is not surprising to us. RD as calculated here includes both large-scale gravitational and non-gravitational effects, and small-scale effects. As can be seen in Figures 4 and 5, there is a large variability in perfusion within an isogravitational plane in these data as evidenced by the standard deviation of the perfusion in any such plane (the width of the grey shaded zones in Figures 4 and 5), and this serves to strongly influence the calculation of RD.

Potential mechanisms of gas exchange improvement in the prone posture

In these normal subjects we saw no change in arterial oxygen saturation as a function of posture, despite seeing marked changes in the distribution of density-normalized perfusion. This is not surprising. In the normal lung in the supine position there is only modest inhomogeneity of V_A/Q (41;42), and so arterial oxygen saturation is well-maintained. Thus, even if improvements in the distribution of perfusion occur, the likely effect in arterial saturation will be minimal or absent. It is likely for that reason that previous studies e.g. (37) have failed to show alterations in gas exchange in normal subjects as a result of a postural change. However

such arguments do not apply in the compromised lung in which lung density is greater, and so in that circumstance one might expect to see changes in gas exchange with posture.

The improvement in the distribution of perfusion in the prone posture compared to supine is more apparent when perfusion is considered as density-normalized perfusion (compare Figures 3B and 3C), and indeed we would argue that this is likely the more appropriate way to consider it. If a perfectly uniform lung were subject to a simple gravitational distortion, one would expect largely parallel changes in both ventilation and perfusion in a given region of the lung; ventilation would be higher in a compressed region of the lung because of a higher regional compliance due to the non-linear P-V curve of the lung. Perfusion per unit volume would be increased because alveoli would be smaller and so more would be in any given volume, and so the net effect on gas exchange would be minimal. Indeed, gravity has been shown to have such an effect on the normal human lung. In microgravity, the distribution of ventilation-perfusion ratio is largely unchanged compared to that measured upright in 1G despite considerable improvements in the underlying distributions of ventilation and perfusion (35). Density-normalized perfusion shows the greatest increase in the prone posture in what was the most dependent lung regions in the supine posture (the posterior lung regions, Figure 3C), those same regions that show the greatest change in density (Figure 3A). Thus, consideration of density-normalized perfusion provides more insight into the effects of a postural change on gas exchange than does perfusion per unit volume alone.

This study shows that, even in the normal lung in which gas exchange in very efficient, as evidenced by a high S_aO_2, a postural change from supine to prone increases pulmonary perfusion, and makes the distribution of pulmonary perfusion more uniform. Both of these effects have the potential to improve gas exchange in the compromised lung. Although extrapolating these results to a compromised lung should be done with caution, they do point to a likely mechanism of the improved oxygenation seen in the prone posture compared to the supine. Posterior lung zones (primarily in the central lung) that were subject to compression in the supine posture have large increases in density-normalized perfusion when the subject moves to the prone posture. This results in a much more uniform distribution of density-normalized perfusion in that posture. There is no corresponding effect in the anterior zone of the lung in the supine posture.

Limitations of this study

Our study focused solely on the perfusion side of pulmonary gas exchange. Clearly gas exchange depends on both ventilation and perfusion. However we would argue that, at least in the normal lung, the compressive effect we describe on perfusion (16) is also applicable to the effect on ventilation (6). Whether such an assertion is valid in a compromised lung is arguable and requires testing.

Like all measurements, our techniques have limitations. We have attempted to correct for technical matters such as coil inhomogeneity and absolute calibration by fixing coil position relative to the subject, correcting for coil inhomogeneity, and incorporating reference phantoms in our imaging protocols. Our measurements are however limited by our ability to acquire data during a breathhold, and also by the need to acquire the perfusion and density images during separate breathholds, which may introduce some error into these measurements, although visual inspection of diaphragmatic position indicated reproducible breath-hold volumes. Further, our density measurements image only free protons (essentially water) and so our distribution of density may be incorrect to the extent that lung tissue that does not contribute to the MRI signal is distributed differently to water in the lung. Finally, our study examined only the right lung to avoid imaging artifacts from the heart on the left side of the chest. We do not however see any reason to suspect less of an effect for the left lung, and indeed there is

evidence for a greater compressive effect on the left lung by the heart when in the supine position (1;23).

Conclusion

In normal humans, a change in posture from supine to prone is associated with an increase in total pulmonary perfusion and an improvement in the distribution of density-normalized perfusion. Specifically, posterior lung zones in the central part of the lung show an increase in density-normalized perfusion in the transition from supine to prone, while anterior lung zones do not show a corresponding increase in the prone to supine transition. These changes likely result from the alleviation of excess compression of the posterior lung in the supine posture when a postural change occurs. We speculate that in the gas exchange compromised lung, these alterations in the distribution of perfusion are an important mechanism of improved oxygenation seen in prone-positioning studies.

Acknowledgements

We thank our subjects for their enthusiastic participation, and acknowledge useful discussions with P.J. Friedman and D.J. Dubowitz.

This work was supported by the National Institutes of Health grants HL081171, HL080203, 1F32-HL078128, and the American Heart Association grant AHA 054002N.

References

1. Albert RK, Hubmayr RD. The prone position eliminates compression of the lungs by the heart. Am J Respir Crit Care Med 2000;161:1660–1665. [PubMed: 10806172]
2. Amis TC, Jones HA, Hughes JMB. Effect of posture on inter-regional distribution of pulmonary ventilation in man. Respir Physiol 1984;56:145–167. [PubMed: 6463423]
3. Bolar DS, Levin DL, Hopkins SR, Frank LF, Liu TT, Wong EC, Buxton RB. Quantification of regional pulmonary blood flow using ASL-FAIRER. Magnetic Resonance in Medicine 2006;55:1308–1317. [PubMed: 16680681]
4. Bone RC. The ARDS lung:New insights from computed tomography. J A M A 1993;269:2134–2135.
5. Brudin LH, Rhodes CG, Valind SO, Wollmer P, Hughes JMB. Regional lung density and blood volume in nonsmoking and smoking subjects measured by PET. J Appl Physiol 1987;63:1324–1334. [PubMed: 3500940]
6. Bryan AC, Milic-Emili J, Pengelly D. Effect of gravity on the distribution of pulmonary ventilation. J Appl Physiol 1966;21:778–784. [PubMed: 5912747]
7. Chang H, Lai-Fook SJ, Domino KB, Schimmel C, Hildebrandt J, Robertson HT, Glenny RW, Hlastala MP. Spatial distribution of ventilation and perfusion in anesthetized dogs in lateral postures. J Appl Physiol 2002;92:762.
8. Chatte G, Sab J, Dubois J, Sirodot M, Gaussorges P, Robert D. Prone position in mechanically ventilated patients with severe acute respiratory failure. Am J Respir Crit Care Med 1997;155:473–478. [PubMed: 9032181]
9. Friedman PJ, Peters RM, Botkin MC, Brimm JE, Meltvedt RC. Estimation of the volume of lung below the left atrium using computed tomography. Critical Care Medicine 1986;14:182–187. [PubMed: 3943333]
10. Gattinoni L, Caironi P, Pelosi P, Goodman LR. What has computed tomography taught us about the acute respiratory distress syndrome? Am J Respir Crit Care Med 2001;164:1701–1711. [PubMed: 11719313]
11. Glenny RW, Polissar L, Robertson HT. Relative contribution of gravity to pulmonary perfusion heterogeneity. J Appl Physiol 1991;71:2449–2452. [PubMed: 1778945]
12. Hakim TS, Lisbona R, Dean GW. Gravity-independent inequality of pulmonary blood flow in humans. J Appl Physiol 1987;63:1114–1121. [PubMed: 3498713]

13. Hatabu H, Alsop DC, Listerud J, Bonnet M, Gefter WB. T2* and proton density measurement of normal human lung parenchyma using submillisecond echo timegradient echo magnetic resonance imaging. Eur J Radiol 1999;29:245–252. [PubMed: 10399610]

14. Henderson AC, Levin DL, Hopkins SR, Olfert IM, Buxton RB, Prisk GK. Steep head-down tilt has perisiting effects on the distribution of pulmonary blood flow. J Appl Physiol 2006;101:583–589. [PubMed: 16601308]

15. Hopkins SR, Garg J, Bolar D, Balouch J, Levin D. Pulmonary blood flow heterogeneity during hypoxia in subjects with prior high altitude pulmonary edema (HAPE). Am J Respir Crit Care Med 2005;171:83–87. [PubMed: 15486339]

16. Hopkins SR, Henderson AC, Levin DL, Yamada K, Arai T, Buxton RB, Prisk GK. Vertical gradients in regional lung densityand perfusion in the human lung: the Slinky effect. J Appl Physiol. 200710.1152/japplphysiol.01289.2006In Press

17. Jones AT, Hansell DM, Evans TW. Pulmonary perfusion in supine and prone positions: an electron-beam computed tomography study. J Appl Physiol 2001;90:1342–1348. [PubMed: 11247933]

18. Kaneko K, Milic-Emili J, Dolovich MB, Dawson A, Bates DV. Regional distribution of ventilation and perfusion as a function of body positon. J Appl Physiol 1966;21:767–777. [PubMed: 5912746]

19. Lamm WJ, Graham MM, Albert RK. Mechanis by which the prone position improves oxygenation in acute lung injury. Am J Respir Crit Care Med 1994;150:184–193. [PubMed: 8025748]

20. Langer M, Mascheroni D, Marcolin R, Gattinoni L. The prone position in ARDS patients: a clinical study. Chest 1988;94:103–107. [PubMed: 3383620]

21. Levin DL, Buxton RB, Speiss JR, Arai T, Balouch J, Hopkins SR. Effects of age on pulmonary perfusion heterogeneity measured by magnetic resonance imaging. J Appl Physiol. 2007In Press

22. Liu S, Margulies SS, Wilson TA. Deformation of the dog lung in the chest wall. J Appl Physiol 1990;68:1979–1987. [PubMed: 2361899]

23. Malbousson LM, Busch CJ, Puybasset L, Lu Q, Cluzel P, Rouby J-J. Role of the heart in the loss of aeration characterizing lower lobes in acute respiratory distress syndrome. CT Scan ARDS Study group. Am J Respir Crit Care Med 2000;161:2005–2012. [PubMed: 10852781]

24. Mayo JR, MacKay A, Whittall K, Baile EM, Pare PD. Measurement of lung water content and pleural pressure gradient with magnetic resonance imaging. J Thoracic Imaging 1995;10:73–81.

25. Milic-Emili J, Henderson JAM, Dolovich MB, Trop D, Kaneko K. Regional distribution of inspired gas in the lung. J Appl Physiol 1966;21:749–759. [PubMed: 5912744]

26. Mure M, Lindahl SG. Prone position improves gas exchange - but how? Acta Anaesth Scand 2001;45:150–159. [PubMed: 11167159]

27. Mure M, Martling CR, Lindahl SG. Dramatic effect on oxygenation in patients with severe acute lung insufficiency treated in the prone position. Critical Care Medicine 1997;25:1539–1544. [PubMed: 9295829]

28. Musch G, Layfield DH, Harris RS, Vidal Melo MF, Winkler T, Callahan RJ, Fischman AJ, Venegas JG. Topographical distribution of pulmonary perfusionand ventilation, assessed by PET in supine and prone humans. J Appl Physiol 2002;98:1841–1851. [PubMed: 12381773]

29. Nyren S, Mure M, Jacobsson H, Larsson SA, Lindahl SG. Pulmonary perfusion is more uniform in the prone than the supine position: scintigraphy in healthy humans. J Appl Physiol 1999;86:1135–1141. [PubMed: 10194194]

30. Pappert D, Rossaint R, Slama K, Gruning T, Falke KJ. Influence of positioning on ventilation-perfusion relationships in severe adult respiratory distress syndrome. Chest 1994;106:1511–1516. [PubMed: 7956412]

31. Pelosi P, D'Andrea L, Vitale G, Pesenti A, Gattinoni L. Vertical gradient of regional lung inflationin adult respiratory distress syndrome. Am J Respir Crit Care Med 1994;149:8–13. [PubMed: 8111603]

32. Pelosi P, Tubiolo D, Mascheroni D, Vicardi P, Crotti S, Valenza F, Gattinoni L. Effects of the prone position on respiratory mechanics and gas exchange during acute lung injury. Am J Respir Crit Care Med 1998;157:387–393. [PubMed: 9476848]

33. Petersson J, Rohdin M, Sanchez-Crespo A, Nyren S, Jacobsson H, Larsson SA, Lindahl SG, Linnarsson D, Glenny RW, Mure M. Paradoxical redistribution of pulmonary blood flow in prone and supine humans exposed to hypergravity. J Appl Physiol 2006;100:240–248. [PubMed: 16150840]

34. Pluim JPW, Maintz JBA, Viergever MA. Mutual-information-based registration of medical images: A survey. Ieee Transactions on Medical Imaging 2003;22:986–1004. [PubMed: 12906253]
35. Prisk GK, Elliott AR, Guy HJB, Kosonen JM, West JB. Pulmonary gas exchange and its determinants during sustained microgravity on Spacelabs SLS-1 and SLS-2. J Appl Physiol 1995;79:1290–1298. [PubMed: 8567575]
36. Richter T, Bellani G, Harris RS, Vidal Melo MF, Winkler T, Venegas JG, Musch G. Effect of prone position on regional shunt, aeration, and perfusion in experimental acute lung injury. Am J Respir Crit Care Med 2005;172:480–487. [PubMed: 15901611]
37. Rohdin M, Petersson J, Sundblad P, Mure M, Glenny RW, Lindahl SG, Linnarsson D. Effects of gravity on lung diffusing capacity and cardiac output in prone and supine humans. J Appl Physiol 2003;95:3–10. [PubMed: 12794090]
38. Rutishauser WJ, Banchero N, Tsakiris AG, Edmundowicz AC, Wood EH. Pleural pressures at dorsal and ventral sites in supine and prone body positions. J Appl Physiol 1966;21:1500–1510. [PubMed: 5923220]
39. Rutishauser WJ, Banchero N, Tsakiris AG, Wood EH. Effect of gravitational ind inertial forces on pleural and esophageal pressures. J Appl Physiol 1967;22:1041–1052. [PubMed: 6027051]
40. Tobin A, Kelly W. Prone ventilation -- it's time. Anaesth Intensive Care 1999;27:194–201. [PubMed: 10212720]
41. Wagner PD, Dantzker DR, Dueck R, Clausen JL, West JB. Ventilation-perfusion inequality in chronic obstructive pulmonary disease. J Clin Invest 1977;59:203–216. [PubMed: 833271]
42. Wagner PD, Laravuso RB, Uhl RR, West JB. Continuous distributions of ventilation-perfusion ratios in normal subjects breathing air and 100% O_2. J Clin Invest 1974;54:54–68. [PubMed: 4601004]
43. West JB, Dollery CT. Distribution of blood flow and ventilation-perfusion ratio in the lung, measured with radioactive CO_2. J Appl Physiol 1960;15:405–410. [PubMed: 13844133]

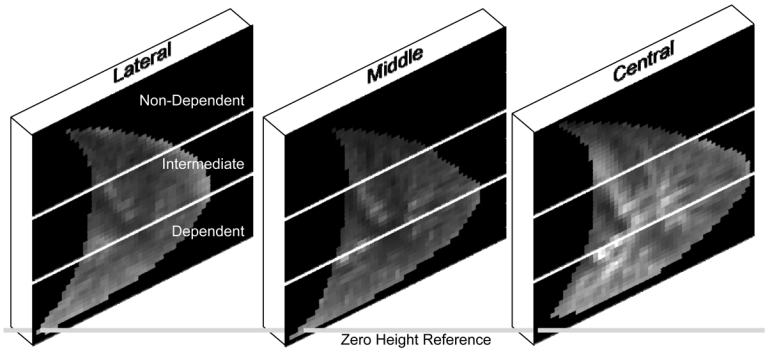

Figure 1.

Representation of the division of slices into gravitational zones. Each 15mm thick adjacent slice was aligned to a common Zero Height Reference taken as the most dependent voxel of lung in the image set. Three vertical zones were then defined as having equal height based on the slice with the greatest anterior-posterior dimension. The same vertical cut point was applied to all three slices. The images shown are lung density images, but the same algorithm also applied to the perfusion and density-normalized perfusion images. See text for details.

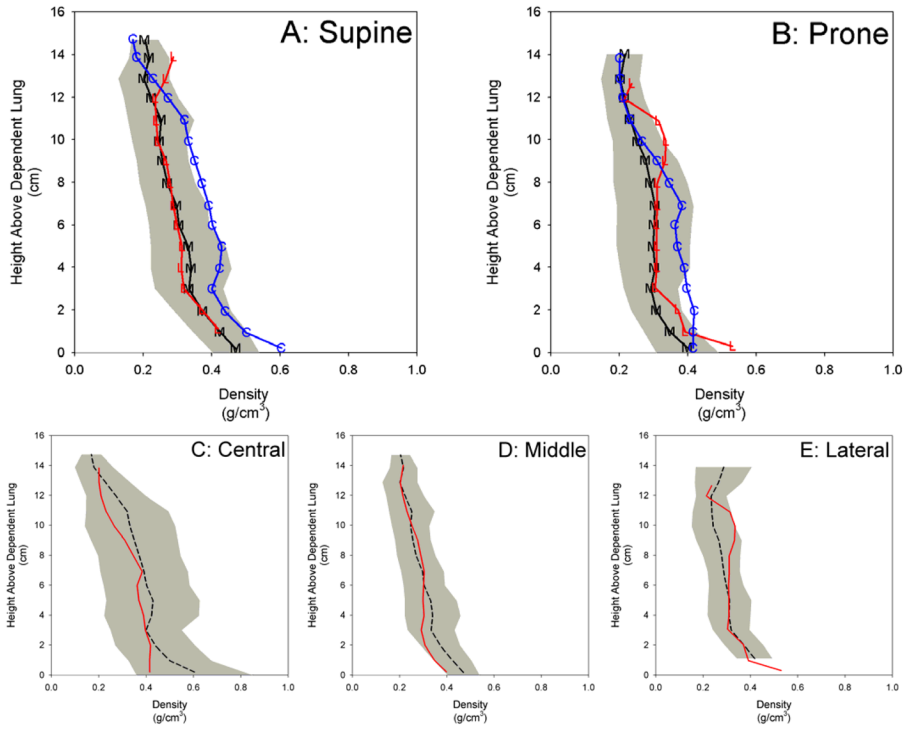

Figure 2.

Lung density in the supine (A) and prone (B) postures for the three sagittal lung slices (central 'C', middle M', and lateral 'L'). Data are plotted with the most gravitationally dependent lung regions at the lowest position. Lines show the average lung density in 1cm high iso-gravitational zones. The grey shaded zone shows mean lung density ± SD for the middle lung slice in panels A & B, and for the supine slice in panels C, D, and E. The SD data from other slices is comparable in magnitude and not shown for clarity. Panels C through E present the lung density plotted in a particular sagittal slice for different posture (supine: dashed line, prone: solid line) for the central, middle and lateral slices respectively. Note that density is plotted as a function of height above the most zero reference point, and so at the bottom of each graph, the supine data represent the most posterior lung zones, while the prone data represent the most anterior lung zones.

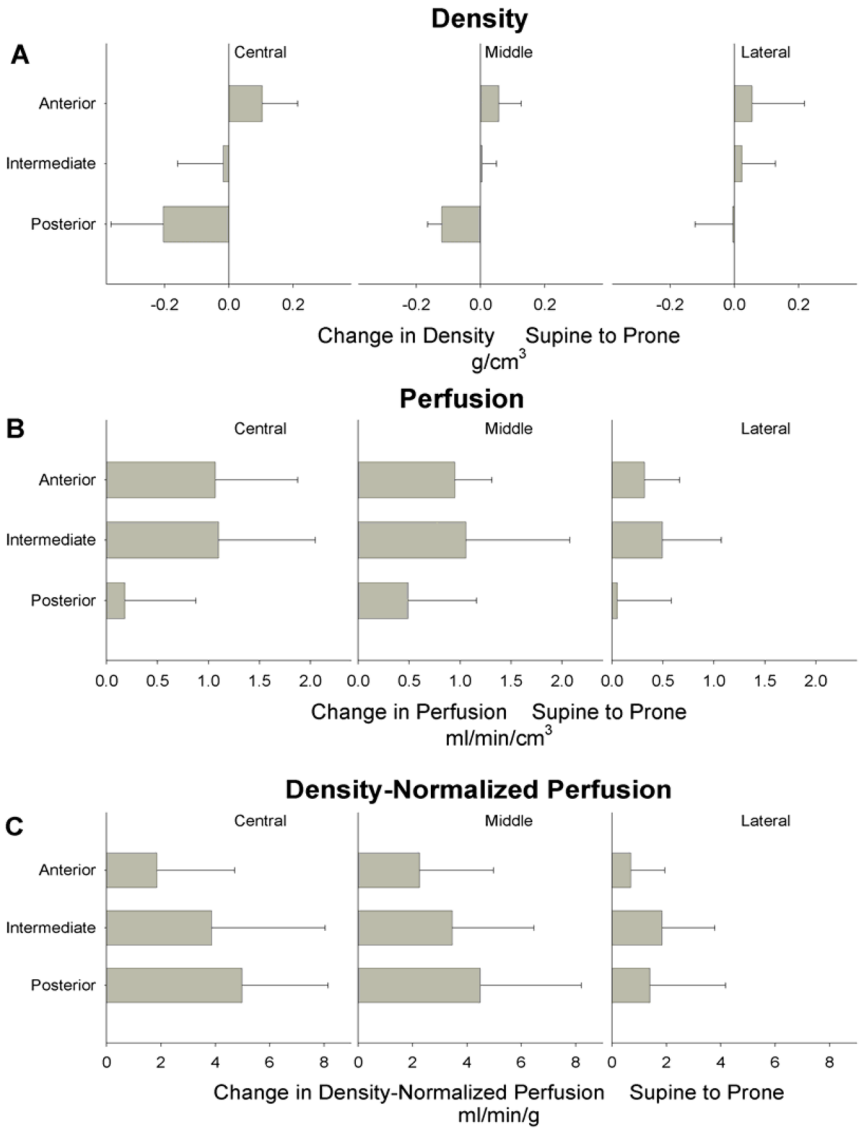

Figure 3.

Change in density (A), perfusion (B) and density normalized perfusion (C) with posture in each of the lung zones. Each lung slice (central, middle, lateral) was divided into gravitationally distinct zone (anterior, intermediate posterior (see text for details)). Values plotted are the change in each variable going from the supine posture to the prone posture, ± SD. For density (A) changes supine to prone were significantly different between lung zones ($P<0.001$), with a significant slice by zone interaction ($P<0.001$), reflecting large shifts in the central ($P<0.0001$) and middle ($P<0.005$), but not in the lateral lung (NS). For perfusion (B) the only significant change was between lung zones ($P=0.006$). For density-normalized perfusion there was a change between zones that was borderline significant ($P=0.077$) with a significant slice by zone interaction ($P=0.043$), reflecting that the changes between zones were significant in the central lung ($P<0.01$) but not in the middle or lateral lung.

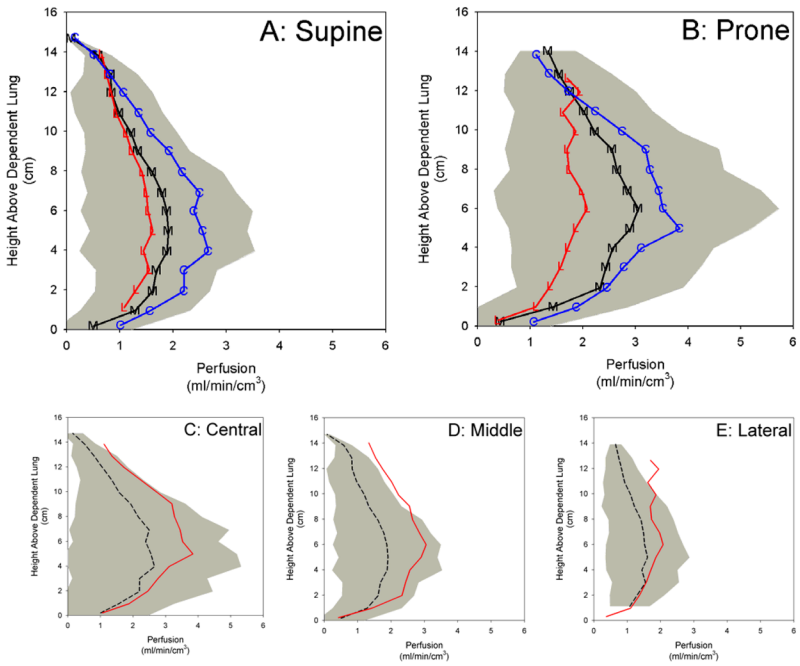

Figure 4.

Pulmonary perfusion in ml/min/cm^3 in the supine (A) and prone (B) postures for the three sagittal lung slices. Panels C through E present the lung density plotted in a particular sagittal slice (central, middle, lateral respectively) for different posture (supine: dashed line, prone: solid line). Figure format same as Figure 2.

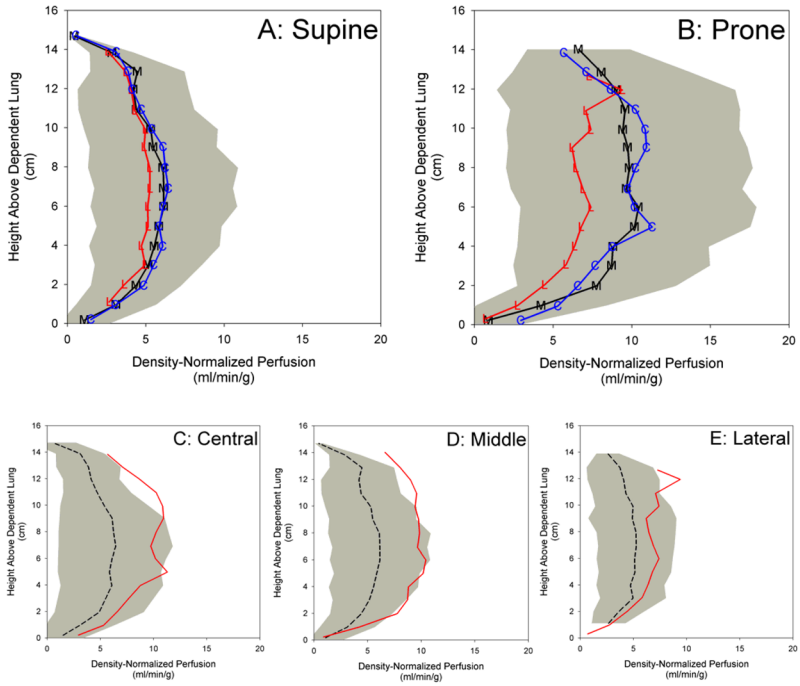

Figure 5.

Density normalized perfusion in ml/min/g in the supine (A) and prone (B) postures for the three sagittal lung slices. Panels C through E present the lung density plotted in a particular sagittal slice (central, middle, lateral respectively) for different postures (supine: dashed line, prone: solid line). Figure format same as Figure 2.

Table 1

Density, perfusion and density-normalized perfusion as a function of posture

Posture	Sagittal Slice	Vertical Region	Lung Density g/cm^3	Blood Flow ml/min/cm^3	Blood Flow/Density ml/min/g
SUPINE					
	Central				
		Anterior	0.305 ± 0.147	1.35 ± 0.60	4.89 ± 1.82
		Intermediate	0.393 ± 0.143	2.47 ± 0.92	6.51 ± 2.50
		Posterior	0.450 ± 0.142	2.09 ± 0.80	4.71 ± 1.20
		Entire Slice	0.383 ± 0.148	1.97 ± 0.88	5.37 ± 2.00
	Middle				
		Anterior	0.246 ± 0.041	1.18 ± 0.52	5.17 ± 2.02
		Intermediate	0.296 ± 0.039	1.76 ± 0.60	6.30 ± 1.90
		Posterior	0.368 ± 0.031	1.59 ± 0.40	4.49 ± 1.05
		Entire Slice	0.304 ± 0.062	1.51 ± 0.54	5.32 ± 1.78
	Lateral				
		Anterior	0.285 ± 0.062	1.15 ± 0.48	4.45 ± 1.71
		Intermediate	0.297 ± 0.034	1.49 ± 0.44	5.13 ± 1.50
		Posterior	0.349 ± 0.031	1.51 ± 0.48	4.47 ± 1.34
		Entire Slice	0.310 ± 0.051	1.38 ± 0.47	4.68 ± 1.45
	Entire Lung		0.332 ± 0.102	1.62 ± 0.69	5.12 ± 1.75
PRONE					
	Central				
		Anterior	0.408 ± 0.162	2.41 ± 0.75	6.74 ± 2.78
		Intermediate	0.375 ± 0.099	3.57 ± 0.87	10.37 ± 3.63
		Posterior	0.245 ± 0.037	2.27 ± 0.44	9.68 ± 2.74
		Entire Slice	0.343 ± 0.127 (NS)	2.75 ±0.89*	8.93 ± 3.31 *
	Middle				
		Anterior	0.303 ± 0.047	2.13 ± 0.58	7.43 ± 2.51
		Intermediate	0.301 ± 0.034	2.82 ± 1.04	9.76 ± 3.83
		Posterior	0.247 ± 0.026	2.08 ± 0.90	8.99 ± 4.40
		Entire Slice	0.284 ± 0.044 (NS)	2.34 ± 0.88 *	8.72 ± 3.59 *
	Lateral				
		Anterior	0.340 ± 0.113	1.47 ± 0.59	5.14 ± 2.66
		Intermediate	0.320 ± 0.100	1.99 ± 0.68	6.97 ± 3.11
		Posterior	0.344 ± 0.166	1.56 ± 0.67	5.85 ± 3.78
		Entire Slice	0.336 ± 0.122 (NS)	1.67 ± 0.65 (NS)	5.99 ± 3.12 (NS)
	Entire Lung		0.320 ± 0.106 (NS)	2.26 ± 0.92 *	7.88 ± 3.55 *

Values are mean ± SD for each defined region of interest (see text for details).

* indicates a significant main effect for slice and posture. See text for zone effects.